Improving the Sensing-Throughput Tradeoff for Cognitive Radios in Rayleigh Fading Channels

Erfan Soltanmohammadi, *Student Member, IEEE,* Mahdi Orooji, *Student Member, IEEE*, Mort Naraghi-Pour *Member, IEEE*

***Abstract*—In-band spectrum sensing in overlay cognitive radio networks requires that the secondary users (SU) periodically suspend their communication in order to determine whether the primary user (PU) has started to utilize the channel. In contrast, in spectrum monitoring the SU can detect the emergence of the PU from its own receiver statistics such as receiver error count (REC). Previously it is shown that in AWGN channels, a hybrid spectrum sensing/spectrum monitoring system significantly improves channel utilization of the SUs and detection delay of the PUs. In this paper we investigate the problem of spectrum monitoring in the presence of fading where the SU employs diversity combining to mitigate the channel fading effects. We show that a decision statistic based on the REC alone does not provide a good performance. Next we introduce new decision statistics based on the REC and the combiner coefficients. It is shown that the new decision statistic achieves significant improvement in the case of maximal ratio combining (MRC). However, for equal gain combining and selection combining the inclusion of combiner coefficients does not improve the performance over REC alone. In the case of MRC we evaluate the receiver operating characteristics from analysis and compare the results with those from simulations using a BCH code as well as a convolutional code. The results show a close match between analysis and simulation results. Channel utilization and detection delay are evaluated from simulations which show that with MRC and the proposed decision statistic, the hybrid spectrum sensing/spectrum monitoring system significantly outperforms spectrum sensing alone.**

***Index Terms*—Spectrum sensing, spectrum monitoring, channel utilization, detection delay, fading channel, diversity combining.**

I. Introduction

Vehicular networks are expected to significantly improve safety and convenience of transportation systems and mitigate traffic congestion by improving road traffic flow. Dynamic spectrum access (DSA) has been proposed for vehicular ad-hoc networks (VANET) to allow access to licensed spectral bands such as TV white spaces [1]–[5]. In particular, in the European "DRiVE" project, DSA is the main focus for spectrum allocation in heterogeneous networks [6].

DSA allows unlicensed secondary users (SU) to utilize the licensed spectral bands that are not in use by the incumbent primary users (PU). Cognitive radio (CR), viewed as the enabling technology for DSA, relies on spectrum sensing (SS) to determine whether a given frequency band is vacant of the PU signal [7]–[9] [1]. Since during their own communication the SUs do not sense the channel, they must periodically suspend their transmission and enter a sensing period so as to determine whether the PU has emerged or not. In order to protect the PU against undue interference from the SUs, stringent requirements are imposed on the detection probability and maximum detection delay of the SS algorithm (see for example [11]). Detection probability can be improved by increasing the duration of the sensing periods and detection delay can be reduced by decreasing the duration of the SU's transmission periods. Both approaches, however, result in reduced throughput in the secondary network.

There is an intricate tradeoff between protection of the PU and the quality of service (QoS) of the SU, referred to as sensing-throughput tradeoff in [12]. In [13], Tang *et al.* evaluate the effect of PU traffic on the SU throughput. In [14], Akin *et al.* assume statistical QoS and maximize the throughput for the SU. To improve the SU's throughput, adaptive scheduling of spectrum sensing to the primary user activities has been investigated in [15] and [16]. These approaches, however, are mainly concerned with spectrum sensing and do not consider the possibility of sensing while the SU is communicating.

It is clear that during the SU's transmissions, the emergence of the PU increases the interference experienced by the SU. This in turn causes a drop in the SU's signal-to-noise (plus interference) ratio (SNR) and it may increase the number of errors in the SU packets. Therefore, while communicating, the SU may attempt to detect the emergence of the PU by monitoring the changes in the receiver's SNR or the number of errors in each received packet. Using this idea, in [17], [18] Boyd *et al.* introduced spectrum monitoring (SM) in which the SU utilizes its receiver statistics to detect the emergence of the PU during the SU's own communication. In [19] we proposed a decision statistic for SM based on the receiver error count (REC)[2] and the output of a cyclic redundancy check (CRC) code and show that for AWGN channels the

The authors are with the Division of Electrical and Computer Engineering, School of Electrical Engineering and Computer Science, Louisiana State University, Baton Rouge, LA 70803 {e-mail: esolta1, morooj1, naraghi@lsu.edu}.

[1]We should point out that this approach is referred to as overlay CR. In contrast, in underlay CR the SU can always access the licensed spectrum provided it can regulate its transmit power so as not to cause harmful interference to the PU. Overlay CR is considered to be more practical since, in contrast to underlay CR, it does not require instantaneous information on the interference channel [10].

[2]REC denotes the number of errors observed in a received packet and is more carefully defined in Section II-A.

proposed algorithm significantly improves the throughput[3] of the SU subject to a maximum PU detection delay.

Using receiver statistics to detect the emergence of the PU would be effective provided that the changes are mainly due to the emergence of the PU (e.g., in the case of AWGN channels). However, this approach may not be effective in the presence of fading in the secondary channel as the changes in the receiver statistics may be due to the variations of the channel rather than the interference from the PU signal. In this paper we investigate the problem of spectrum monitoring in the case that the secondary channel experiences flat Rayleigh fading. We first show that approaches which are based on the REC alone do not perform well. Next we consider the use of a multi-antenna system to improve the performance of spectrum monitoring. Multi-antenna systems in conjunction with diversity combining have been widely used in wireless communication to combat the deleterious effects of channel fading. Recently, multi-antenna systems have also been proposed for SS where it is shown that they can significantly improve the performance of SS techniques [20]–[24]. We assume that the SU uses a multi-antenna system along with one of three diversity combining techniques, namely maximal ratio combining (MRC), equal gain combining (EGC), or selective combining (SC). We introduce a new decision statistic based on the REC, a CRC code and the combiner statistics. The performance of this new decision statistic is evaluated in terms of detection and false alarm probabilities, channel utilization and detection delay. We also simulate the proposed system using two forward error correcting codes, namely a BCH code and a convolutional code. It is shown that the results from these simulations are closely matched with those from analysis.

The rest of this paper is organized as follows. The system model and problem formulation are presented in Section II. The decision statistic using REC, CRC and combiner statistics is introduced and analyzed in Section III. Numerical results are presented in Sections IV and conclusions are drawn in Section V.

II. System Model and Problem Formulation

The SU starts with a spectrum sensing interval (SSI) of duration T_s during which it senses the channel. If at the end of an SSI the channel is found to be occupied, another SSI begins[4] and this continues until the SU finds the channel to be vacant. At this time a spectrum monitoring interval (SMI) begins during which the SU transmits a maximum of K_M packets. After the reception of each packet the SU computes a decision statistic (described below) in order to detect whether the PU has emerged in the in-band channel. If it is decided that the PU has emerged, the SU terminates the SMI and enters the spectrum sensing phase. Otherwise the channel is deemed to be vacant and the SU continues its packet transmission. To allow for periodic sensing of the channel the SU terminates an SMI after the transmission of (at most) K_M packets and starts a new SSI.

Let H_η denote the hypothesis of interest where $\eta = 0$ and 1 correspond to the absence and the presence of the PU signal, respectively. We assume that the SU receiver is equipped with $L \geq 1$ identical antenna branches and that, as in [25], the L branches experience identically distributed, uncorrelated flat fading. The nth received symbol at the lth branch of the SU under H_η is given by,

$$r_{l,n} = s_n h_l + v_{l,n} + \eta u_{l,n}, l = 1, 2, \cdots, L, n = 1, 2, \cdots \quad (1)$$

where $\{s_n\}$ is the sequence of SU's transmitted symbols, $\{v_{l,n}\}_{l=1}^{L}$ denote L independent, identically distributed (i.i.d.) circularly symmetric Gaussian noise processes with zero mean and variance $\mathcal{E}_v$, and for $k \neq l$, $\{v_{k,n}\}$ and $\{v_{l,n}\}$ are independent, and $\{u_{l,n}\}$ denotes the sequence of primary user symbols at the lth branch of the SU receiver. We assume that the PU symbols $\{u_{l,n}\}$ have undergone independent flat fading which is not explicitly shown but is included in the symbols $\{u_{l,n}\}$. Finally, $\{h_l\}_{l=1}^{L}$, which denote the (secondary) channel fading coefficients, are i.i.d. circularly symmetric Gaussian random variables with mean zero and variance 1, i.e., $h_l \sim \mathcal{CN}(0, 1)$. Let $\alpha_l \triangleq |h_l|$ and let $\theta_l \triangleq \angle h_l$.

We assume linear combining in the SU receiver where the output of the combiner is given by,

$$r_n \triangleq \sum_{l=1}^{L} w_l r_{l,n} \quad (2)$$

and where w_l, $l = 1, 2, \cdots, L$ are the combiner weighting coefficients which are determined by the diversity combining technique [26]. Table I shows the values of w_l for the three combining techniques MRC, EGC, and SC.

A. Decision Statistic

At the SU transmitter the information sequence is first encoded using a CRC code (for error detection) followed by a forward error correction (FEC) scheme to obtain an N-bit packet. A block diagram of the receiver is shown in Fig. 1 (with the switch $\mathcal{S}$ open for now) where the received packet is demodulated and decoded. The decoded packet is then checked by the CRC and also encoded using a replica of the transmitter's encoder. The encoder output is compared to the output of the demodulator[5] to calculate the number of errors referred to as REC and denoted by e in the following. Note that the actual number of errors in a packet, subsequently denoted by k, is not always available in the receiver. In particular, when the packet is not decoded correctly, then $e \neq k$ and therefore the value of k is unknown to the receiver. However, if the packet is decoded correctly, then $k = e$.

Remark 1. *In today's communication systems FEC and CRC are in widespread use to combat channel errors and to verify whether the packet is correctly decoded or not, respectively [27]. Therefore there is no loss of throughput due to FEC if it is already in use by the SU; moreover, the throughput loss due*

[3]In this paper we have used the notions of *throughput* and *channel utilization* interchangeably to refer to the average fraction of time that the SU is able to use the channel when the PU is absent.

[4]We should point out that the results presented here will not change if the SU moves to another channel once it finds the current channel to be occupied.

[5]If the decoder uses soft decision, then hard decision must be performed on the demodulator output before comparison with the encoder's output.

TABLE I

COMBINER-WEIGHTS, INSTANTANEOUS SNR, AND ITS DISTRIBUTION FOR MAXIMAL RATIO COMBINING (MRC), EQUAL GAIN COMBINING (EGC) AND SELECTION COMBINING (SC) TECHNIQUES. IN THE TABLE, $\gamma_{b,\eta}$ IS THE AVERAGE SNR OF THE RECEIVED SIGNAL PER BRANCH UNDER H_η AND $\mathcal{E}_r^{(l)}$ IS THE ENERGY OF THE RECEIVED PACKET FOR THE l^{TH} BRANCH.

Diversity	w_l	$p_{\gamma_\eta}(x)$	γ_η
MRC	h_l^*	$\frac{1}{(L-1)!\gamma_{b,\eta}^L} x^{(L-1)} e^{\frac{-x}{\gamma_{b,\eta}}}$	$\sum_{l=1}^{L} \gamma_\eta^{(l)}$
EGC	$e^{-j\theta_l}$	L=2: $\frac{1}{\gamma_{b,\eta}} e^{\frac{-2x}{\gamma_{b,\eta}}} - \sqrt{\pi} e^{\frac{-x}{\gamma_{b,\eta}}}$ $\times \left(\frac{1}{2\sqrt{x\gamma_{b,\eta}}} - \sqrt{\frac{x}{\gamma_{b,\eta}^3}} \right)$ $\times \left(1 - 2Q\sqrt{2x/\gamma_{b,\eta}}\right)$,	$\frac{(\sum_{i=1}^{L} \alpha_l)^2 \gamma_{b,\eta}}{L}$
SC	$\begin{cases} 1 & \mathcal{E}_r^{(l)} > \mathcal{E}_r^{(k)}, \forall k \neq l \\ 0 & \text{otherwise} \end{cases}$	$\frac{L}{\gamma_{b,\eta}} \left(1 - e^{-x/\gamma_{b,\eta}}\right)^{(L-1)}$ $\times e^{-x/\gamma_{b,\eta}}$	$\max\left\{\gamma_\eta^{(1)}, \ldots, \gamma_\eta^{(L)}\right\}$

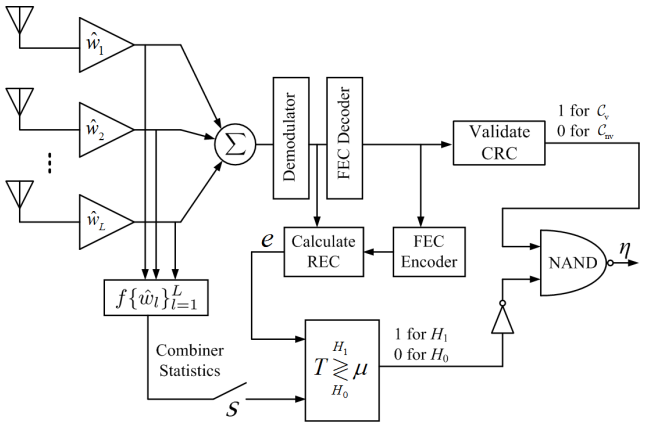

Fig. 1. Proposed model using demodulator statistics and combiner statistics.

to the addition of CRC is very small considering the number of CRC bits compared to the length of a packet.

Denote by $\mathcal{C}_{\text{v}}$ and $\mathcal{C}_{\text{nv}}$ the events that the CRC is validated and not validated, respectively. The decision statistic in SMI is defined by,

$$T^{(\text{REC})} \cong \begin{cases} \left(\{e \geq \mu^{(\text{REC})}\} \cap \mathcal{C}_{\text{v}}\right) \cup \mathcal{C}_{\text{nv}}, & \text{Decide } H_1 \\ \text{Otherwise}, & \text{Decide } H_0 \end{cases} \quad (3)$$

where $\mu^{(\text{REC})}$ is the REC threshold which is chosen not to exceed $t^{(\text{FEC})}$, the maximum number of errors in a packet that the FEC is able to correct. The decision statistic in (3) indicates the emergence of the PU if the CRC is not validated, or if the CRC is validated and the REC e exceeds the threshold $\mu^{(\text{REC})}$. As (3) indicates, the decision statistic in not a function of the actual number of errors k.

If the packet is decoded correctly, then the CRC will correctly identify this event ($\mathcal{C}_{\text{v}}$) and in this case $e = k$. On the other hand if the decoder fails, then either the CRC will identify this event ($\mathcal{C}_{\text{nv}}$) or the CRC fails to identify the decoder failure ($\mathcal{C}_{\text{v}}$). In the former case the SMI will be terminated. However, in the latter case when the packet is not decoded correctly and the CRC also fails to identify this event, the proposed SM scheme may fail for the current packet. Consequently the SMI may be terminated when PU is not present (resulting in loss of channel utilization for the SU) or it may be continued when PU is present (resulting in increased detection delay). It is shown in [28] that for large packets (e.g. $N > 100$) the probability of failure for an $L-$bit CRC is approximately 2^{-L}. (Thus for the commonly used CRCs such as CCITT-16, CRC-32-Castagnoli and CRC-32-IEEE [29]–[31], the probability of CRC failure is around 1.5×10^{-5} and 2.3×10^{-10}, respectively.) It is shown in [19] that the increase in detection delay due to the CRC failure is less than $2^{-L} \times T_p$ seconds and the loss in channel utilization for the SU is less than $2^{-L} \times \frac{T_s}{T_s + K_M \times T_p} < 2^{-L}$, where T_p is the packet transmission time. In light of this, in the following we ignore the event of a decoder failure followed by a CRC failure.

If $\mathcal{C}_{\text{nv}}$ occurs, then the received packet is not correctly decoded (decoder failure). So, $\mathcal{C}_{\text{nv}}$ implies that $k \geq t^{(\text{FEC})} \geq \mu^{(\text{REC})}$. On the other hand (ignoring the event that the decoder and the CRC both fail), $\mathcal{C}_{\text{v}}$ implies that the packet is correctly decoded. Thus from (3) we get

$$\begin{aligned} & p\left(\left(\{e \geq \mu^{(\text{REC})}\} \cap \mathcal{C}_{\text{v}}\right) \cup \mathcal{C}_{\text{nv}}\right) \\ & = p\left(\left(\{k \geq \mu^{(\text{REC})}\} \cap \mathcal{C}_{\text{v}}\right) \cup \left(\{k \geq \mu^{(\text{REC})}\} \cap \mathcal{C}_{\text{nv}}\right)\right) \\ & = p(\{k \geq \mu^{(\text{REC})}\}) \end{aligned} \quad (4)$$

Therefore, (3) is equivalent to,

$$T^{(\text{REC})} = k \underset{H_0}{\overset{H_1}{\gtrless}} \mu^{(\text{REC})}. \quad (5)$$

The probabilities of false alarm and detection in SMI are given by $p_f = p(\{k \geq \mu^{(\text{REC})}\} \mid H_0)$ and $p_d = p(\{k \geq \mu^{(\text{REC})}\} \mid H_1)$, respectively.

It is shown in [23] that, if the modulation scheme of the PU is a constant modulus scheme such as MPSK, then after undergoing Rayleigh fading, the received PU sequences $\{u_{l,n}\}$, for $l = 1, 2, \cdots, L$ are i.i.d. zero-mean circularly symmetric complex Gaussian (CSCG) random processes. This model is also accurate if the PU uses orthogonal frequency division multiplexing (OFDM) [22]. For other modulation

schemes with a large constellation this assumption is approximately true [23], [32]. Therefore we model $\{u_{l,n}\}$ as a zero-mean CSCG random process with variance $\mathcal{E}_u$. This model is assumed merely to make the analysis tractable and the proposed decision statistic does not depend on this assumption. Other articles using this model include [12] and [33].

From the SU receiver point of view, the PU signal during SMI is an additive noise. So the SNR for branch l under H_η is given by,

$$\gamma_\eta^{(l)} \triangleq \frac{|h_l|^2 \mathcal{E}_s}{\mathcal{E}_v + \eta \mathcal{E}_u} \tag{6}$$

where $\mathcal{E}_s$ is the energy of the SU transmitted signal. Note that for a given packet this SNR is fixed.

In the SU receiver, the signals from different branches are combined. Let $\gamma_\eta, \eta = 0, 1$, denote the SNR at the output of the combiner and let $p_{\gamma_\eta}(x)$ denotes its probability density function. Table I shows γ_η and $p_{\gamma_\eta}(x)$ for different combining techniques [34]. To find the number of bits in error in a packet of length N, we assume that the SU uses BPSK modulation. The results can be extended to other modulation scheme in an straightforward manner by substituting the probability of bit error corresponding to the modulation of interest. The probability of k errors in a packet of length N under H_η can now be written as

$$\begin{aligned} p_k(k|H_\eta) &= E_{\gamma_\eta}[p_k(k|\gamma_\eta, H_\eta)] \\ &= \int_0^\infty \binom{N}{k} p_b(x)^k (1 - p_b(x))^{N-k} p_{\gamma_\eta}(x)\, dx \end{aligned} \tag{7}$$

where $p_b(\gamma_\eta)$ is the bit error probability for SNR γ_η.

Fig. 2 shows the receiver operating characteristic (ROC) curves (p_d vs. p_f) obtained from analysis as described above as well as from simulation for three cases of MRC, EGC and SC. The average SNR per branch under H_0 and H_1 is fixed and equal to 2 dB and 0.6 dB, respectively. In the case of EGC and for $L > 2$ branches, $p_{\gamma_\eta}(x)$ cannot be written in closed form [34]. Therefore, the performance is only evaluated from simulations. For comparison we also show the ROC curves for the decision statistic in (3) over AWGN channel and for the same SNR values. As Fig. 2 shows, while $T^{(\text{REC})}$ is effective in detecting the emergence of the PU in AWGN channels, in the case of fading channels its performance deteriorates significantly. This degradation is expected and is due to the fact that $T^{(\text{REC})}$ cannot determine whether an increase in the number of errors in a packet is due to the interference from the PU signal or is caused by channel fading. This result implies that for fading channels, using the REC alone as a test statistic may not provide acceptable performance even when diversity techniques are used. Hence, alternative decision statistics are needed.

B. Channel Estimation

The probability in (7) is derived assuming that the combiner weighting coefficients $w_l, l = 1, 2, \cdots, L$ are derived from precise knowledge of the channel coefficients $h_l, l = 1, 2, \cdots, L$. However, in practice the channel coefficients have to be estimated and there is always an error between the estimated channel coefficients and their actual values. In general, channel estimation error is caused by two distinct channel impairments [35]. One is due to the decorrelation of the pilots from the signal due to distinct distortions that the channel imparts on them because of their separation in time or frequency. The second is due to noise. It can be seen that the first phenomenon affects the channel estimation in the same manner whether the PU is present (H_1) or not (H_0). The estimation error due to noise, however, will be different as the SU experiences more noise when PU is present due to the interference from the PU signal.

Denote by $\hat{h}_l = \hat{\alpha}_l e^{j\hat{\theta}_l}$ the estimated channel coefficient corresponding to h_l. As in [25] we assume that the channel estimation errors, defined by $\ell_l \triangleq \hat{h}_l - h_l$, are independent of the channel coefficients h_l, and that $\{\ell_l\}_{l=1}^L$ are independent and identically distributed (i.i.d.) circularly symmetric complex Gaussian random variables. Given the hypothesis H_η, the complex correlation coefficient ϱ_η between h_l and $\hat{h}_l$ and its magnitude denoted by ρ_η are defined by

$$\begin{aligned} \varrho_\eta &\triangleq \frac{E[h_l \hat{h}_l^* | H_\eta]}{\sqrt{E[|h_l|^2] E[|\hat{h}_l|^2 | H_\eta]}} = \varrho_\eta^R + j \varrho_\eta^I \\ \rho_\eta^2 &\triangleq |\varrho_\eta|^2 = (\varrho_\eta^R)^2 + (\varrho_\eta^I)^2, \quad \eta = 0, 1. \end{aligned} \tag{8}$$

where here and subsequently, superscripts R and I represent the real and imaginary parts, respectively. From the assumptions on $\{h_l\}_{l=1}^L$ and $\{\ell_l\}_{l=1}^L$ we conclude that the estimated channel coefficients $\{\hat{h}_l\}_{l=1}^L$ are also i.i.d. circularly symmetric Gaussian random variables and conditioned on H_η,

$$\hat{h}_l | H_\eta \sim \mathcal{CN}(0, 2 - \rho_\eta^2) \quad \text{for} \quad l = 1, 2, \cdots, L, \tag{9}$$

where by $X|\Lambda \sim \mathcal{CN}(m, \sigma^2)$ we denote the conditional distribution of X given Λ. Finally we have $\text{var}(\ell_l | H_\eta) = \text{var}(h)(1 - \rho_\eta^2)$.

In the case of imperfect channel estimation, it is shown in [25] that the probability of observing a bit in error is identical to the case of perfect channel estimation with effective SNR $\gamma_\eta^{(\text{eff})} \triangleq (\varrho_\eta^R)^2 \gamma_\eta / (1 + \gamma_\eta (1 - \rho_\eta^2))$. Consequently, when weighting coefficients are not perfectly estimated, the performance of the proposed decision statistic will be equivalent to that of a system with a lower SNR.

III. Decision Statistics Using Error Counts and Combiner Coefficients

We saw in the previous section that the REC is not a good indicator of the presence or absence of the PU signal. Therefore, in our decision statistic we would like to augment the REC with the channel state information (CSI) that is available in the SU receiver in the form of the combiner coefficients. To emphasize the fact that the combiner coefficients are obtained from an estimate of the CSI (rather than the exact values), in the following we denote the combiner coefficients by $\hat{w}_l, l = 1, 2, \cdots, L$ and let $\hat{\mathbf{w}} = (\hat{w}_1, \hat{w}_2, \cdots, \hat{w}_L)$. We define a new decision statistic as follows.

$$T \cong \begin{cases} \left(\left\{ \frac{p(e, f(\hat{\mathbf{w}}) | H_1)}{p(e, f(\hat{\mathbf{w}}) | H_0)} \geq \mu \right\} \cap \mathcal{C}_{\text{v}} \right) \cup \mathcal{C}_{\text{nv}}, & \text{Decide } H_1 \\ \text{Otherwise}, & \text{Decide } H_0 \end{cases} \tag{10}$$

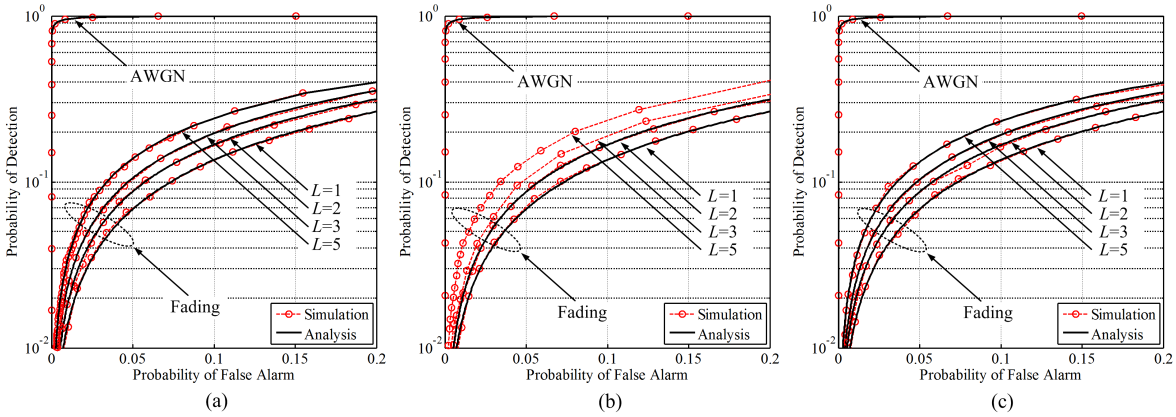

Fig. 2. Comparison between the performance of $T^{(\mathrm{REC})}$ in AWGN channel and fading channel for different number of antennas, L, and different diversity techniques for $N = 1024$, $\gamma_{b,0} = 2$ dB and $\gamma_{b,1} = 0.6$ dB and BPSK signaling. (a): Maximal Ratio Combining, $T^{(\mathrm{REC})}_{\mathrm{MRC}}$, (b): Equal Gain Combining, $T^{(\mathrm{REC})}_{\mathrm{EGC}}$ (c): Selection Combining, $T^{(\mathrm{REC})}_{\mathrm{SC}}$.

where $f(\hat{\mathbf{w}})$ is a function of the combiner coefficients to be determined for each diversity scheme. Fig. 1 (with the switch $\mathcal{S}$ closed) shows the proposed model. Similar to the approach from (3) to (5), one can show that[6] when $t^{(\mathrm{FEC})} \geq \mu$,

$$T = \frac{p(k, f(\hat{\mathbf{w}}) \mid H_1)}{p(k, f(\hat{\mathbf{w}}) \mid H_0)} \underset{H_0}{\overset{H_1}{\gtrless}} \mu \ . \tag{11}$$

While the receiver implements the decision rule in (10), for our analysis an in order to determine the function $f(.)$ for each combining method, we consider (11) in the following.

A. Maximal Ratio Combining

It is well known that MRC is the optimum diversity technique in the sense of maximizing the output SNR of the combiner [36]. In the case of imperfect channel estimation, the combiner coefficients are given by $\hat{w}_l = \hat{h}_l^*$. To evaluate the decision statistic in (11), we first find the joint probability of observing k errors and an estimated channel fading vector $\underline{\hat{h}} \triangleq (\hat{h}_1, \hat{h}_2, \cdots, \hat{h}_L)$ given H_η, i.e.,

$$p(k, \underline{\hat{h}}|H_\eta) = p(k|\underline{\hat{h}}, H_\eta) p(\underline{\hat{h}}|H_\eta) \tag{12}$$

We have

$$p(\underline{\hat{h}}|H_\eta) = \prod_{l=1}^{L} p(\hat{h}_l^R|H_\eta) p(\hat{h}_l^I|H_\eta), \tag{13}$$

From (9) and the fact that $\hat{h}_l$'s are i.i.d., we get

$$p(\underline{\hat{h}}|H_\eta) = \frac{1}{\left[2\pi(1-\rho_\eta^2/2)\right]^L} \exp\left(-\frac{\sum_{l=1}^{L} |\hat{h}_l|^2}{2(1-\rho_\eta^2/2)}\right) \tag{14}$$

To find $p(k|\underline{\hat{h}}, H_\eta)$, let

$$\psi \triangleq \frac{\mathrm{Re}\left(\sum_{l=1}^{L} h_l \hat{h}_l^*\right)}{\sqrt{\sum_{l=1}^{L} |\hat{h}_l|^2}}. \tag{15}$$

[6]Ignoring the event that the decoder and the CRC both fail.

Then,

$$\begin{aligned} p(k|\underline{\hat{h}}, H_\eta) &= \int_{-\infty}^{\infty} p(k|\psi, \underline{\hat{h}}, H_\eta) p(\psi|\underline{\hat{h}}, H_\eta) d\psi \\ &= \int_{-\infty}^{\infty} \binom{N}{k} [P(E|\psi, \underline{\hat{h}}, H_\eta)]^k [1 - P(E|\psi, \underline{\hat{h}}, H_\eta)]^{N-k} \\ &\quad \times p(\psi|\underline{\hat{h}}_\eta, H_\eta) \ d\psi \end{aligned} \tag{16}$$

where $P(E|\psi, \underline{\hat{h}}, H_\eta)$ is the bit error probability given $\psi, \underline{\hat{h}}$ and H_η and is given by, [25]

$$P(E|\psi, \underline{\hat{h}}, H_\eta) = Q\left(\psi\sqrt{2\gamma_\eta}\right) \tag{17}$$

Moreover, it is shown in Appendix A that,

$$\psi|\underline{\hat{h}}, H_\eta \sim \mathcal{N}\left(\frac{\sqrt{\sum_{l=1}^{L} |\hat{h}_l|^2}}{2-\rho_\eta^2} \ , \ \frac{1-\rho_\eta^2}{2(2-\rho_\eta^2)}\right) \tag{18}$$

By substituting (17) and (18) into (16), we get,

$$\begin{aligned} p(k|\underline{\hat{h}}, H_\eta) = \int_{-\infty}^{\infty} \binom{N}{k} Q^k(\psi\sqrt{2\gamma_\eta})(1 - Q(\psi\sqrt{2\gamma_\eta}))^{N-k} \\ \times \frac{1}{\sqrt{\pi\left(\frac{1-\rho_\eta^2}{2-\rho_\eta^2}\right)}} \ e^{-\frac{(\hat{\mathcal{A}} - (2-\rho_\eta^2)\psi)^2}{(1-\rho_\eta^2)(2-\rho_\eta^2)}} \ d\psi \end{aligned} \tag{19}$$

where

$$\hat{\mathcal{A}} \triangleq \sqrt{\sum_{l=1}^{L} |\hat{h}_l|^2}. \tag{20}$$

Substituting (14), (19), and (20) into (12), we get $p(k, \underline{\hat{h}}|H_\eta)$.

From (14) and (19) it is evident that $p(k, \underline{\hat{h}}|H_\eta)$ depends only on $\hat{\mathcal{A}}$ and not the values of individual $\hat{h}_l$'s. All combinations of the estimated channel coefficients $\hat{h}_1, \hat{h}_2, \cdots, \hat{h}_L$ which result in the same value for $\hat{\mathcal{A}}$ are observed with equal probability at the SU. Consequently, in the case of MRC,

instead of $(k, \underline{\hat{h}})$ it is sufficient to use the pair $(k, \hat{\mathcal{A}})$ in the decision statistic. Thus we let $f(\hat{\mathbf{w}}) \triangleq \hat{\mathcal{A}}$ and define our decision statistic by

$$T_{\text{MRC}} \triangleq \frac{p(k, \hat{\mathcal{A}} \mid H_1)}{p(k, \hat{\mathcal{A}} \mid H_0)} \underset{H_0}{\overset{H_1}{\gtrless}} \mu^{(\text{MRC})} \tag{21}$$

where $\mu^{(\text{MRC})} \leq t^{(\text{FEC})}$ is the threshold in the case of MRC. Analysis of this rule requires $p(k, \hat{\mathcal{A}}|H_\eta)$ which can be obtained from $p(k, \underline{\hat{h}}|H_\eta)$. From (14) and (19) we see that $p(k, \underline{\hat{h}}|H_\eta)$ depends only on $||\underline{\hat{h}}||$. Letting $\Xi_\eta(k, ||\underline{\hat{h}}||) \triangleq p(k, \underline{\hat{h}}|H_\eta)$ we get

$$p(k, \hat{\mathcal{A}}|H_\eta) = \Xi_\eta(k, \hat{\mathcal{A}}) S_{2L}(\hat{\mathcal{A}}) \tag{22}$$

where

$$S_n(r) = \frac{2\pi^{n/2}}{\Gamma(n/2)} r^{n-1} \tag{23}$$

is the surface area of the n-dimensional hyper-sphere of radius r [37]. Evaluation of (22) requires the computation of the integral in (19). In Appendix B an approximation for $p(k, \hat{\mathcal{A}}|H_\eta)$ is derived in closed form which does not involve any integration. The accuracy of this approximation is verified by comparing in Section IV the performance results from analysis (using this approximation) with simulation results.

For an intuitive explanation of the proposed decision rule in (21), consider the 2D space of $e \in \mathbb{N},\ 0 \leq e \leq N$, and $\hat{\mathcal{A}} \in \mathbb{R}^+$ which is split into two decision regions, Ω_0 and Ω_1 associated with H_0 and H_1, respectively. Fig. 3 demonstrates two examples of these decision regions when $\gamma_0 = 6$ dB, $\gamma_1 = 0$ dB, $\rho_0 = 0.95$, $\rho_1 = 0.85$, $N = 256$ and $L = 2$ antennas are employed in the MRC combiner. The two decision boundaries are plotted for the false alarm probabilities of $p_f = 0.01$ and 0.05 and the corresponding detection probabilities, $p_d = 0.73$ and 0.86, respectively. In each case the area under the curve shows Ω_0 and the area above the curve shows Ω_1. Note that when the SU experiences large fades (small $\hat{\mathcal{A}}$), it expects to observe a large number of errors per packet due to fading alone. Therefore, as demonstrated in Fig. 3, in this case only for a very large number of errors a decision is made in favor of H_1. On the other hand when fading is small (large $\hat{\mathcal{A}}$), only a few errors per packet can be attributed to fading. As a result, in this case even for a small number of errors a decision is made in favor of H_1. This is how the inclusion of $\hat{\mathcal{A}}$ in the decision statistic improves the performance of spectrum monitoring over fading channels.

By defining the decision regions (Ω_0 and Ω_1), and from (21), the probabilities of false alarm and detection in the case of MRC are given by,

$$p_f^{(\text{MRC})} \triangleq \sum \int_{(k,\hat{\mathcal{A}}) \in \Omega_1} p(k, \hat{\mathcal{A}}|H_0)\ d\hat{\mathcal{A}} \tag{24}$$

$$p_d^{(\text{MRC})} \triangleq \sum \int_{(k,\hat{\mathcal{A}}) \in \Omega_1} p(k, \hat{\mathcal{A}}|H_1)\ d\hat{\mathcal{A}} \tag{25}$$

B. Equal Gain Combining

In equal gain combining we first co-phase the signals on individual branches and then combine them with equal magnitude. Therefore in this case the combiner coefficients are given by $\hat{w}_l = e^{-j\hat{\theta}_l}$ where $\hat{\theta}_l$ is the estimated phase of the fading coefficient on branch l. Consequently, we define the decision statistic by

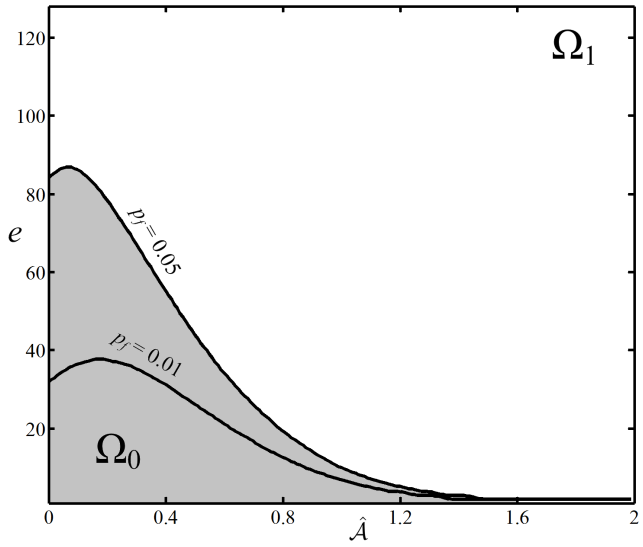

Fig. 3. The decision regions for T_{MRC} when $N = 256$, $L = 2$, $\gamma_0 = 6$ dB, $\gamma_1 = 0$ dB, $\rho_0 = 0.95$, $\rho_1 = 0.85$, and $(p_f, p_d) = (0.01, 0.73)$ and $(0.05, 0.86)$.

$$T_{\text{EGC}} = \frac{p(k, f(\underline{\hat{\theta}})|H_1)}{p(k, f(\underline{\hat{\theta}})|H_0)} \underset{H_0}{\overset{H_1}{\gtrless}} \mu^{(\text{EGC})} \tag{26}$$

where $\underline{\hat{\theta}} \triangleq (\hat{\theta}_1, \hat{\theta}_2, \cdots, \hat{\theta}_L)$. Towards deriving the decision statistic we consider the following joint distribution.

$$p(k, \underline{\hat{\theta}}|H_\eta) = p(k|\underline{\hat{\theta}}, H_\eta) p(\underline{\hat{\theta}}|H_\eta) \tag{27}$$

It is well known that the estimated channel phases $\hat{\theta}_1, \hat{\theta}_2, \cdots, \hat{\theta}_L$ are i.i.d. and uniformly distributed over $[0, 2\pi)$, Therefore,

$$p(\underline{\hat{\theta}}|H_\eta) = \prod_{l=1}^{L} p(\hat{\theta}_l|H_\eta) = (\frac{1}{2\pi})^L,$$
$$0 \leq \hat{\theta}_l < 2\pi, \quad \text{for } l = 1, 2, \cdots, L. \tag{28}$$

To evaluate $p(k|\underline{\hat{\theta}}, H_\eta)$ let

$$\zeta \triangleq \frac{\text{Re}\left(\sum_{l=1}^{L} h_l e^{-j\hat{\theta}_l}\right)}{\sqrt{L}}. \tag{29}$$

Then by conditioning on ζ, we get

$$p(k|\underline{\hat{\theta}}, H_\eta) = \int_{-\infty}^{\infty} p(k|\zeta, \underline{\hat{\theta}}, H_\eta)\ p(\zeta|\underline{\hat{\theta}}, H_\eta)\ d\zeta$$
$$= \binom{N}{k} \int_{-\infty}^{\infty} [P(E|\zeta, \underline{\hat{\theta}}, H_\eta)]^k\ [1 - P(E|\zeta, \underline{\hat{\theta}}, H_\eta)]^{N-k}$$
$$\times\ p(\zeta|\underline{\hat{\theta}}, H_\eta)\ d\zeta \tag{30}$$

It is shown in [25] that,

$$P(E|\zeta, \underline{\hat{\theta}}, H_\eta) = Q(\zeta\sqrt{2\gamma_\eta}) \tag{31}$$

which is independent of $\hat{\underline{\theta}}$. Moreover, it is proven in Appendix C that given H_η, ζ is independent of $\hat{\underline{\theta}}$, i.e., $p(\zeta|\hat{\underline{\theta}}, H_\eta) = p(\zeta|H_\eta)$. From this we conclude that $p(k|\hat{\underline{\theta}}, H_\eta) = p(k|H_\eta)$. Finally from (27), (28) we get,

$$p(k, \hat{\underline{\theta}}|H_\eta) = p(k|H_\eta) \tag{32}$$

So, the decision statistic in the case of EGC is then given by

$$T_{\text{EGC}} = \frac{p(k, f(\hat{\underline{\theta}})|H_1)}{p(k, f(\hat{\underline{\theta}})|H_0)} = \frac{p(k|H_1)}{p(k|H_0)} \tag{33}$$

This shows that, in the case of EGC, the estimated phases cannot help us decide whether an increase in the REC at the SU is due to fading or the emergence of the PU signal. In light of (28), this result in fact makes intuitive sense. We conclude that in the presence of fading, EGC diversity technique is not a good option for spectrum monitoring in a fading channel. This is also demonstrated by the simulation results in Section IV.

C. Selection Combining

In selection combining, all the weighting coefficients are zero except for the branch with the highest SNR for which the coefficient is one. Therefore in this case the weighting coefficients do not provide any information about the emergence of the primary user. In other words,

$$p(\{\hat{w}_l\}_{l=1}^L \mid H_0) = p(\{\hat{w}_l\}_{l=1}^L \mid H_1). \tag{34}$$

Therefore in this case

$$T_{\text{SC}} = \frac{p(k, f(\{\hat{w}_l\}_{l=1}^L) \mid H_1)}{p(k, f(\{\hat{w}_l\}_{l=1}^L) \mid H_0)} = \frac{p(k \mid H_1)}{p(k \mid H_0)} \tag{35}$$

Similar to EGC, the CSI from SC combining method does not enhance the performance of spectrum monitoring over the REC alone.

Remark 2. *We need to discuss the complexity associated with the proposed spectrum monitoring method. As pointed out in [18], receiver statistics such as REC are useful in adaptive transmission protocols where modulation, coding or transmit power may be adjusted in order to mitigate the effects of time-varying channel and interference. If REC is already being collected by the receiver, then no significant additional hardware is required by the proposed method. If not, then the receiver is required to implement the CRC check, the FEC encoder and the hypothesis testing as shown in Fig. 1. The hardware and computational complexity of CRC and the FEC encoder is not very high particularly in comparison with the complexity of the rest of the SU receiver including multiple RF chains for diversity combining, the demodulator and the decoder. Hypothesis testing requires the computation of T in* (11) *for which $p(k, f(\hat{\boldsymbol{w}}) \mid H_\eta)$, $\eta = 0, 1$, is needed. In the case of MRC, we evaluate an accurate approximation for $p(k, f(\hat{\boldsymbol{w}}) \mid H_\eta)$ in Appendix B which alleviates the need for computation of integrals. In summary the incremental complexity of the proposed method for the SU receiver is not significant.*

IV. Numerical Results

In this section we provide performance results from simulation and analysis to asses the effectiveness of the proposed spectrum monitoring methods. We should point out that our goal here is to demonstrate the advantage of a hybrid spectrum sensing/spectrum monitoring system over a system that uses spectrum sensing alone. Therefore we are not concerned with the specific spectrum sensing method that is being used and only need to assume its probabilities of detection and false alarm which, subsequently, are denoted by $\hat{p}_d$ and $\hat{p}_f$, respectively.

Simulation results are obtained by running at least 10^4 independent trials, and analytical results of the proposed spectrum monitoring for MRC is obtained using the approximation in Appendix B. The length of the spectrum sensing interval is identical to the length of a packet, and the transmitter uses BPSK modulation with rate 2 Mbps. In the simulations Jakes' model [38] with the sum of sinusoids is used to model a flat Rayleigh fading channel. In particular, we use 16 sinusoids for the Jakes' model with the maximum Doppler frequency of 90 Hz (corresponding to a mobile speed of 54 Km/h and the carrier frequency of 1.8 GHz).

Fig. 4 compares the ROC curve of the proposed decision statistic for MRC (T_{MRC}) to three other cases which use diversity combining but make their SM decisions based only on the REC alone. These three cases are MRC, EGC and SC denoted by $T_{\text{MRC}}^{(\text{REC})}$, $T_{\text{EGC}}^{(\text{REC})}$, and $T_{\text{SC}}^{(\text{REC})}$, respectively. A remark is in order here. Although the latter three cases use only REC to detect the presence of the PU signal, their performance is not identical as seen in Fig. 4. This is due to the fact that since the combining techniques are different, the REC's (under each hypothesis) are also different in these three cases.

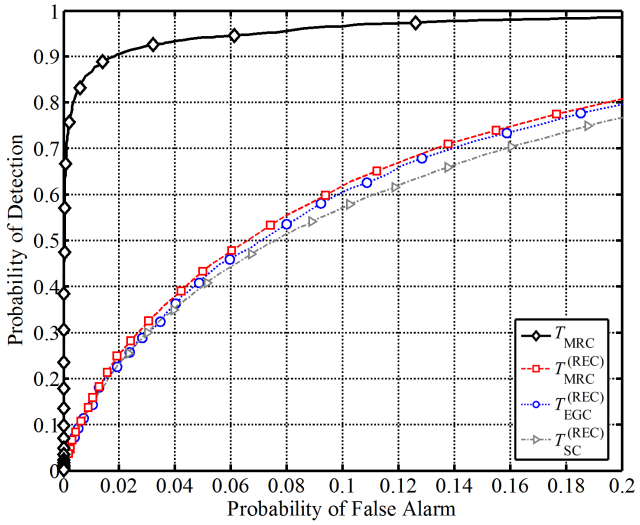

Fig. 4. Comparison from simulations between T_{MRC}, $T_{\text{MRC}}^{(\text{REC})}$, $T_{\text{EGC}}^{(\text{REC})}$, and $T_{\text{SC}}^{(\text{REC})}$ for $N = 1024$, $\gamma_0 = 2$ dB, $\gamma_1 = -2$ dB, $\rho_0 = 0.95$, $\rho_1 = 0.85$, and $L = 4$.

As expected, T_{MRC} outperforms the other three test statistics. For example for probability of false alarm $p_f = 0.1$, the probability of detection for T_{MRC} is .97 whereas it is below .62 in the other cases. Due to the fact that the performance of

$T_{\text{MRC}}^{(\text{REC})}$, $T_{\text{EGC}}^{(\text{REC})}$ and $T_{\text{SC}}^{(\text{REC})}$ are close to each other (see Figs. 2 and 4), in the following we only consider the decision statistic $T_{\text{MRC}}^{(\text{REC})}$ for our comparisons.

Channel utilization for the SUs and detection delay of the PUs can be used to evaluate the efficacy of the hybrid spectrum sensing/spectrum monitoring systems. As described previously, channel utilization is defined as the average fraction of time that under hypothesis H_0 the SU communicates over the channel. Detection delay is the average time it takes to detect the presence of the primary user after it emerges in the channel. Using Markov chain models in [19] we evaluated channel utilization and detection delay for a hybrid spectrum sensing/spectrum monitoring technique for AWGN channel. For AWGN channels, the event of observing k errors is independent from packet to packet, and so Markov models can be employed. In contrast, in the case of fading channels, the fading coefficients affecting consecutive packets are correlated (in time). As a result the decision statistics are also correlated and the Markov model is not applicable. We have not been able to obtain closed form formulas for channel utilization and detection delay in the case of fading channels. The following results are obtained from extensive simulations.

Figs. 5 and 6 show channel utilization and detection delay of T_{MRC} and $T_{\text{MRC}}^{(\text{REC})}$ versus the detection probability p_d of spectrum monitoring for packet length $N = 1024$, number of antennas $L = 2$, $\gamma_0 = 2$ dB, $\gamma_1 = -2$ dB, $\rho_0 = 0.95$, $\rho_1 = 0.85$, and the probabilities of false alarm and detection for the spectrum sensing method $(\hat{p}_f, \hat{p}_d) = (.1, .9)$, for different values of K_M.

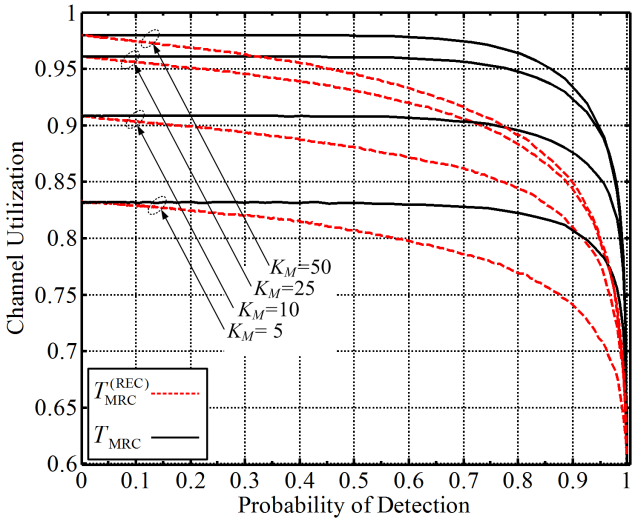

Fig. 5. Channel utilization versus the probability of detection for T_{MRC} and $T_{\text{MRC}}^{(\text{REC})}$, $N = 1024$, $L = 2$, $\gamma_0 = 2$ dB, $\gamma_1 = -2$ dB, $\rho_0 = 0.95$, $\rho_1 = 0.85$, $f_{\text{m}} = 90$Hz, $(\hat{p}_f, \hat{p}_d) = (0.1, 0.9)$ and K_M= 5, 10, 25, and 50.

Channel utilization is a decreasing function of false alarm probability p_f owing to the fact that the portion of time that the SU has a chance to access the channel decreases with p_f. Since p_d is an increasing function of p_f, channel utilization is also a decreasing function of p_d. Channel utilization increases with the duration of the spectrum monitoring interval (K_M). This is due to the fact that, for a fixed spectrum sensing interval, as K_M increases, the fraction of time that the SU is able to transmit also increases resulting in increased throughput for the SU. However, increasing K_M will also increase detection delay. The reason is that for equal probabilities of false alarm for spectrum monitoring and spectrum sensing, spectrum sensing has a higher probability of detection. Since increasing K_M (for fixed spectrum sensing intervals) reduces the fraction of time the SU spends in spectrum sensing, detection delay increases with K_M.

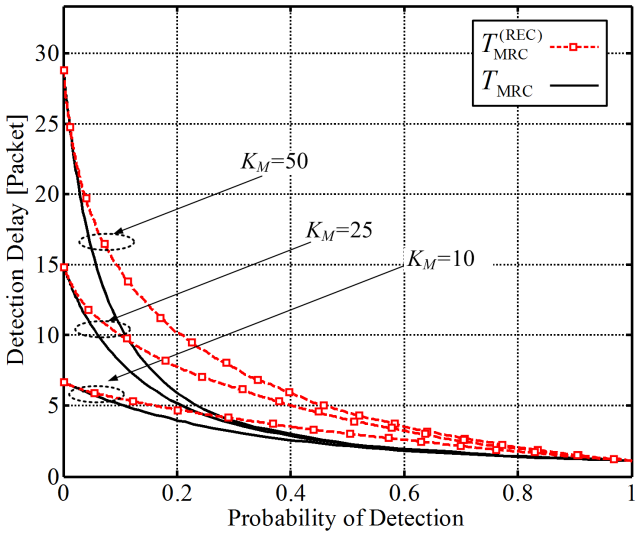

Fig. 6. Detection delay versus the probability of detection for T_{MRC} and $T_{\text{MRC}}^{(\text{REC})}$, $N = 1024$, $L = 2$, $\gamma_0 = 2$ dB, $\gamma_1 = -2$ dB, $\rho_0 = 0.95$, $\rho_1 = 0.85$, $(\hat{p}_f, \hat{p}_d) = (0.1, 0.9)$ and $f_{\text{m}} = 90$Hz.

Figs. 5 and 6 also show that T_{MRC} significantly outperforms $T_{\text{MRC}}^{(\text{REC})}$ for the same value of p_d. One should note that, to obtain the same value of p_d, $T_{\text{MRC}}^{(\text{REC})}$ requires significantly higher SNR than T_{MRC} as evident from the ROC curves in Fig. 4.

In Fig. 7 we plot channel utilization versus detection delay p_d for the hybrid spectrum sensing/spectrum monitoring techniques using T_{MRC} and $T_{\text{MRC}}^{(\text{REC})}$ for different values of K_M and L. The performance of the spectrum sensing alone is also shown. It can be seen that the hybrid technique significantly outperform spectrum sensing alone. As illustrated by this figure, for any given channel utilization and fixed K_M, spectrum sensing is equivalent to the hybrid system with $p_d = p_f = 0$, and has the maximum detection delay. Moreover, the decision statistic T_{MRC}, outperforms $T_{\text{MRC}}^{(\text{REC})}$. For example for $K_M = 25$, channel utilization of 95% can be achieved by T_{MRC} and $T_{\text{MRC}}^{(\text{REC})}$ resulting in detection delays of 1.5 and 8.2 packets, respectively.

Fig. 8 shows the ROC curves for T_{MRC} for different number of branches, L. The simulation results are obtained for a SU which uses one of two error-correcting codes. The first is a rate $1/2$ convolutional code with the generator matrix $[g^{(0)} = (716502)_8 \ ; \ g^{(1)} = (514576)_8]$, [39]. The second code is a $(1023, 503)$ binary BCH code with rate $503/1023 \approx 1/2$. We also employed the CRC-8 code with the generator polynomial $x^8+x^7+x^6+x^4+x^2+1$. As the plots illustrate the simulation results using actual coding schemes closely match the results from analysis. Note that for $L = 1$, there is no diversity and $\hat{A} = |\hat{h}|$. As L increases to 2, the performance improves.

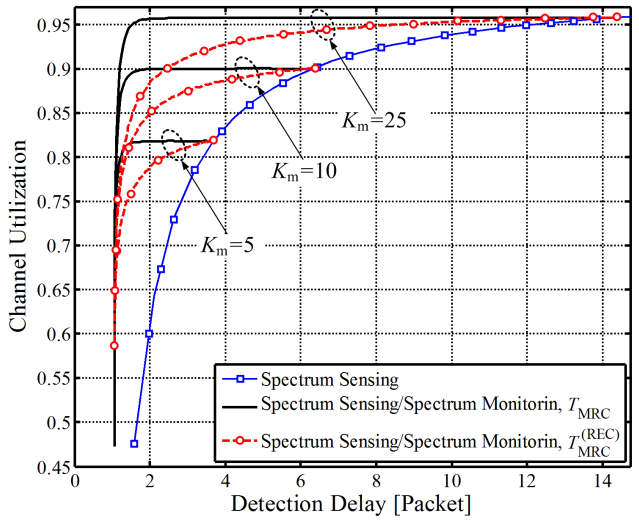

Fig. 7. Channel utilization versus detection delay for T_{MRC} and $T_{\text{MRC}}^{(\text{REC})}$, $N = 1024$, $L = 2$, $\gamma_0 = 2$ dB, $\gamma_1 = -2$ dB, $\rho_0 = 0.95$, $\rho_1 = 0.85$, $(\hat{p}_f, \hat{p}_d) = (0.1, 0.9)$ and $f_{\text{m}} = 90$Hz .

However, for $L = 3$ the performance starts to degrade and for $L = 10$ the ROC is close to the chance line, i.e. $p_f = p_d$. This behavior is due to the fact that as L increases the SNR at the output of the combiner improves and the REC is reduced. For very large values of L the emergence of the PU does not cause a significant change in the SNR or the REC. Therefore in such cases it is difficult for the decision statistic to detect the emergence of the PU. In Appendix D we present a method for the judicious selection of the number of antennas L. For the parameters in Fig. 8, (74) results in $\tilde{L} = 2.56$ from which we get $L_{\text{opt}} = \left\lfloor \tilde{L} \right\rfloor = 2$. This matches the result in Fig. 8.

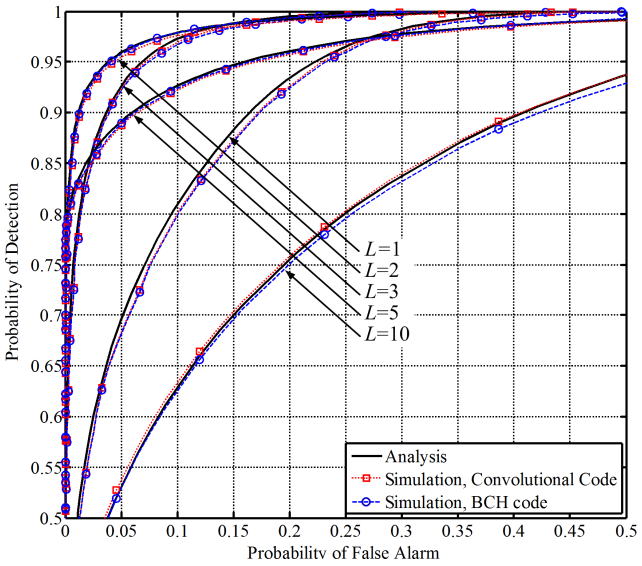

Fig. 8. ROC for the proposed decision statistic T_{MRC} for $N = 1024$, $\gamma_0 = 6$ dB, $\gamma_1 = 0$ dB, $\rho_0 = 0.9$ and $\rho_1 = 0.8$ for $L = 1, 2, 3, 5, 10$.

Fig. 9 shows detection delay versus channel utilization for different number of branches and K_M when $N = 256$, $\gamma_0 = 4$ dB, $\gamma_1 = -1$ dB, $\rho_0 = 0.9$ and $\rho_1 = 0.8$. This figure also shows that the performance improves from $L = 1$ to $L = 4$ but it degrades as L increases to 10. From (74) we get $\tilde{L} = 3.2$ and $L_{\text{opt}} = \left\lceil \tilde{L} \right\rceil = 4$.

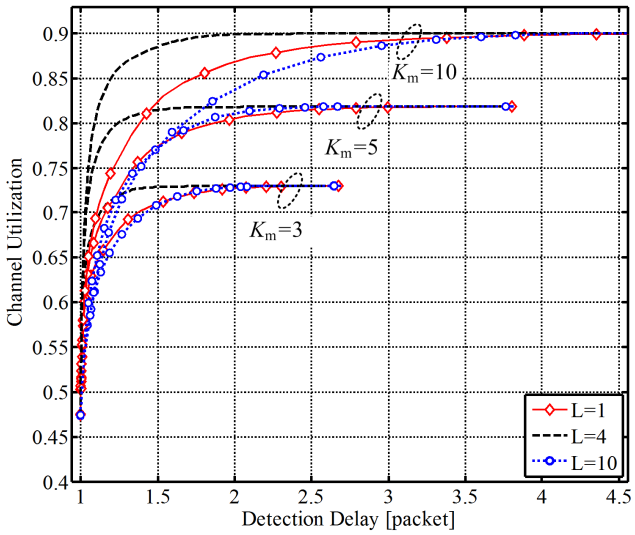

Fig. 9. Channel utilization versus detection delay for T_{MRC}, $N = 256$, $\gamma_0 = 4$ dB, $\gamma_1 = -1$ dB, $\rho_0 = 0.9$, $\rho_1 = 0.8$, $K_M = 5, 10$ and $L = 1, 4, 10$.

V. Conclusions

In this paper we investigate the problem of spectrum monitoring over Rayleigh fading channels. It is assumed that the secondary user is equipped with multiple antennas and uses diversity combining to mitigate the effects of fading. We consider maximal ratio combining, equal gain combining and selection combining. It is shown that spectrum monitoring using REC alone is not as effective in the case of fading channels as it is in the case of AWGN channels. Next we introduce new decision statistics based on the REC and the combiner coefficients for the three combining schemes. It is shown that only in the case of MRC the combiner coefficients improve the decision statistic over the REC alone. Numerical results are presented to compare the performance of the hybrid spectrum sensing/spectrum monitoring technique with spectrum sensing alone. The results show that the proposed decision statistic significantly outperforms the decision statistic using REC alone. Moreover the hybrid spectrum sensing/spectrum monitoring significantly outperforms spectrum sensing alone.

Appendix

A. Evaluation of $p(\psi|\underline{\hat{h}}, H_\eta)$

First let us find $p_{h_l^R|\hat{h}_l^R}(x|y, H_\eta)$. We have

$$p_{h_l^R|\hat{h}_l^R}(x|y, H_\eta) = \frac{p_{\hat{h}_l^R|h_l^R}(y|x, H_\eta) p_{h_l^R}(x)}{p_{\hat{h}_l^R}(y, H_\eta)} = \frac{p_{\ell_l^R}(y - x|H_\eta) p_{h_l^R}(x)}{p_{\hat{h}_l^R}(y|H_\eta)} \tag{36}$$

Note that h_l^R is independent of the hypothesis H_η. It is discussed in section II that, ℓ_l and h_l are two independent

zero-mean circular Gaussian random variables. Thus

$$h_l^R \text{ and } h_l^I \quad \sim \mathcal{N}(0, 1/2) \tag{37}$$

$$\ell_l^R|H_\eta \text{ and } \ell_l^I|H_\eta \sim \mathcal{N}(0, 1/2 - \rho_\eta^2/2) \tag{38}$$

$$\hat{h}_l^R|H_\eta \text{ and } \hat{h}_l^I|H_\eta \sim \mathcal{N}(0, 1 - \rho_\eta^2) \tag{39}$$

By substituting (37), (38), and (39) into (36) and after some manipulations one can show that,

$$h_l^R|\hat{h}_l^R, H_\eta \sim \mathcal{N}\left(\frac{\hat{h}_l^R}{2-\rho_\eta^2}\ ,\ \frac{1-\rho_\eta^2}{2(2-\rho_\eta^2)}\right) \tag{40}$$

Similarly the distribution of $h_l^I|\hat{h}_l^I, H_\eta$ can be derived. From (40) we can write,

$$\frac{\hat{h}_l^R h_l^R}{\sqrt{\sum_{l=1}^L |\hat{h}_l|^2}}\ \Bigg|\ \hat{h}_l, H_\eta \tag{41}$$

$$\sim \mathcal{N}\left(\frac{(\hat{h}_l^R)^2}{(2-\rho_\eta^2)(\sqrt{\sum_{l=1}^L |\hat{h}_l|^2})}, \frac{(1-\rho_\eta^2)(\hat{h}_l^R)^2}{2(2-\rho_\eta^2)(\sum_{l=1}^L |\hat{h}_l|^2)}\right)$$

and in the same way, one can rewrite (41) for the imaginary parts. Let us rewrite ψ in (15) as,

$$\psi = \frac{\text{Re}\left(\sum_{l=1}^L h_l \hat{h}_l^*\right)}{\sqrt{\sum_{l=1}^L |\hat{h}_l|^2}} = \frac{\sum_{l=1}^L \left(h_l^R \hat{h}_l^R + h_l^I \hat{h}_l^I\right)}{\sqrt{\sum_{l=1}^L |\hat{h}_l|^2}} \tag{42}$$

Then (41) and (42) imply that,

$$\psi|\underline{\hat{h}}, H_\eta \sim \mathcal{N}\left(\frac{\sqrt{\sum_{l=1}^L |\hat{h}_l|^2}}{2-\rho_\eta^2}\ ,\ \frac{1-\rho_\eta^2}{2(2-\rho_\eta^2)}\right) \tag{43}$$

B. The approximation of $p(k, \hat{\mathcal{A}}|H_\eta)$

To make a decision on the hypothesis, the integral in (16) should be evaluated and multiplied by (14) and (23).

For $0 < k < N$, let us approximate,

$$\binom{N}{k} Q^k(x)(1-Q(x))^{N-k} \approx a e^{-\frac{(x-m)^2}{2\sigma^2}} \tag{44}$$

where m, a and σ are the solutions of following equations,

$$\binom{N}{k} Q^k(x)(1-Q(x))^{N-k}\big|_{x=m} = a \tag{45}$$

$$\binom{N}{k} Q^k(x)(1-Q(x))^{N-k}\Big|_{x=m} = 0 \tag{46}$$

$$\binom{N}{k} Q^k(x)(1-Q(x))^{N-k}\Big|_{x=m} = -\frac{a}{\sigma^2} \tag{47}$$

Equations (45), (46) and (47) give

$$m = Q^{-1}(\frac{k}{N}) \tag{48}$$

$$a = \binom{N}{k} \frac{k^k (N-k)^{N-k}}{N^N} \tag{49}$$

$$\sigma^2 = 2\pi \frac{k^2}{N^2}(\frac{1}{k} - \frac{1}{N}) \exp\left((Q^{-1}(\frac{k}{N}))^2\right) \tag{50}$$

where Q^{-1} is inverse Q-function.

For cases $k = 0$ and $k = N$, the left hand-side of (44) is equal to $(1-Q(x))^N$ and $Q^N(x)$, respectively, which are approximated by $U(x-m_0)$ and $1-U(x-m_N)$, respectively, where $U(.)$ is the unit step-function, and m_0 and m_N are the solutions of following equations,

$$(1-Q(x))^N\big|_{x=m_0} = \frac{1}{2} \tag{51}$$

$$Q^N(x)\big|_{x=m_N} = \frac{1}{2} \tag{52}$$

This gives,

$$(1-Q(x))^N \approx U(x - Q^{-1}(1 - \sqrt[N]{1/2})) \tag{53}$$

$$Q^N(x) \approx 1 - U(x - Q^{-1}(\sqrt[N]{1/2})) \tag{54}$$

By substituting (44), (53), and (54) into (19), $p(k|\underline{\hat{h}}, H_\eta)$ is approximated by

$$p(k|\underline{\hat{h}}, H_\eta) \approx \tag{55}$$

$$\begin{cases} \frac{1}{\sqrt{2\pi\acute{\sigma}_\eta^2}} \int_{m_0}^{\infty} e^{\frac{-(\acute{m}_\eta - x)^2}{2\acute{\sigma}_\eta^2}}\ dx, & k = 0 \\ \frac{a}{\sqrt{2\pi\acute{\sigma}_\eta^2}} \int_{-\infty}^{\infty} e^{-\frac{(\acute{m}_\eta - x)^2}{2\acute{\sigma}_\eta^2} - \frac{(m-x)^2}{2\sigma^2}}\ dx, & 0 < k < N \\ \frac{1}{\sqrt{2\pi\acute{\sigma}_\eta^2}} \int_{-\infty}^{m_N} e^{\frac{-(\acute{m}_\eta - x)^2}{2\acute{\sigma}_\eta^2}}\ dx, & k = N \end{cases}$$

where $\acute{m}_\eta \triangleq \frac{\hat{\mathcal{A}}\sqrt{2\gamma_\eta}}{2-\rho_\eta^2}$ and $\acute{\sigma}_\eta^2 \triangleq \gamma_\eta \frac{1-\rho_\eta^2}{2-\rho_\eta^2}$. Approximation of $p(k|\underline{\hat{h}}, H_\eta)$ in (55) is found by considering that,

$$\int_x^\infty e^{-t^2/2}\ dt = \sqrt{2\pi}\ Q(x) \tag{56}$$

$$\int_{-\infty}^{\infty} e^{-(b_2 t^2 + b_1 t + b_0)}\ dt = \sqrt{\frac{\pi}{b_2}}\ e^{\frac{b_1^2 - 4b_2 b_0}{4b_2}} \tag{57}$$

Finally by substituting the approximation of $p(k|\underline{\hat{h}}, H_\eta)$ into (12), $p(k, \hat{\mathcal{A}}|H_\eta)$ is approximated by (58). Comparision between the simulation results and analysis results (see Fig. 8) shows the accuracy of this approximation.

$$p(k, \hat{\mathcal{A}}|H_\eta) \approx \tag{58}$$

$$\begin{cases} Q\left(\frac{Q^{-1}(1-\sqrt[N]{1/2}) - \acute{m}_\eta}{\acute{\sigma}_\eta}\right) \frac{2\hat{\mathcal{A}}^{(2L-1)} e^{-\hat{\mathcal{A}}^2/(2-\rho_\eta^2)}}{(2-\rho_\eta^2)^L (L-1)!}, & k = 0 \\ \frac{a\acute{\sigma}_\eta}{\sqrt{\sigma^2 + \acute{\sigma}_\eta^2}} \exp[\frac{-(m-\acute{m}_\eta)^2}{2(\sigma^2+\acute{\sigma}_\eta^2)}] \frac{2\hat{\mathcal{A}}^{(2L-1)} e^{-\hat{\mathcal{A}}^2/(2-\rho_\eta^2)}}{(2-\rho_\eta^2)^L (L-1)!}, & 0 < k < N \\ \left[1 - Q\left(\frac{Q^{-1}(\sqrt[N]{1/2}) - \acute{m}_\eta}{\acute{\sigma}_\eta}\right)\right] \frac{2\hat{\mathcal{A}}^{(2L-1)} e^{-\hat{\mathcal{A}}^2/(2-\rho_\eta^2)}}{(2-\rho_\eta^2)^L (L-1)!}, & k = N \end{cases}$$

C. Proof of Independence of ζ and $\underline{\hat{\theta}}$

The goal is to prove $p(\zeta|\underline{\hat{\theta}}, H_\eta) = p(\zeta|H_\eta)$. Let us rewrite

$$\zeta = \sum_{l=1}^L z_l \tag{59}$$

where

$$z_l \triangleq \frac{\mathrm{Re}\left(h_l e^{-j\hat{\theta}_l}\right)}{\sqrt{L}} = \frac{h_l^R \cos\hat{\theta}_l + h_l^I \sin\hat{\theta}_l}{\sqrt{L}} \tag{60}$$

Since $\{h_l\}_{l=1}^L$ are i.i.d. random variables, given $\underline{\hat{\theta}}$ and H_η the distribution of ζ is the convolution of the distribution of $z_1, z_2, \ldots, z_l$. Besides,

$$p(z_l|\hat{\theta}_l, H_\eta) = \int_{-\infty}^{\infty} p(z_l|\hat{\theta}_l, \hat{\alpha}_l, H_\eta)\ p(\hat{\alpha}_l|\hat{\theta}_l, H_\eta)\ d\hat{\alpha}_l \tag{61}$$

Since $\hat{h}$ is circularly symmetric Gaussian, its magnitude, $\hat{\alpha}$, is Rayleigh distributed and is independent of its angle, $\hat{\theta}$. Thus

$$p(\hat{\alpha}_l = x|\hat{\theta}_l, H_\eta) = p(\hat{\alpha}_l = x|H_\eta) = \frac{2x}{2-\rho_\eta^2} e^{-\frac{x^2}{2-\rho_\eta^2}} \tag{62}$$

Moreover, from

$$\begin{aligned} h_l^R &= \hat{\alpha}_l \cos\hat{\theta}_l - \ell_l^R \\ h_l^I &= \hat{\alpha}_l \sin\hat{\theta}_l - \ell_l^I, \end{aligned} \tag{63}$$

we get

$$\begin{aligned} h_l^R|\hat{\alpha}, \hat{\theta}, H_\eta &\sim \mathcal{N}\left(\frac{\hat{\alpha}\cos\hat{\theta}}{2-\rho_\eta^2}, \frac{1-\rho_\eta^2}{2(2-\rho_\eta^2)}\right) \\ h_l^I|\hat{\alpha}, \hat{\theta}, H_\eta &\sim \mathcal{N}\left(\frac{\hat{\alpha}\sin\hat{\theta}}{2-\rho_\eta^2}, \frac{1-\rho_\eta^2}{2(2-\rho_\eta^2)}\right), \end{aligned} \tag{64}$$

which implies that,

$$z_l|\hat{\theta}_l, \hat{\alpha}_l, H_\eta \sim \mathcal{N}\left(\frac{\hat{\alpha}_l}{\sqrt{L}(2-\rho_\eta^2)}, \frac{1-\rho_\eta^2}{2L(2-\rho_\eta^2)}\right). \tag{65}$$

It can be seen that for any given $\hat{\theta}$ the last distribution is Gaussian with mean and variance which are independent of $\hat{\theta}$. Substituting (62) and (65) into (61) and after some manipulations we get

$$\begin{aligned} &p_{z_l|\hat{\theta}_l}(x|y, H_\eta) = p_{z_l}(x|H_\eta) \\ &= \frac{1}{\sqrt{\pi\frac{2-\rho_\eta^2}{1-\rho_\eta^2}}}\ e^{\frac{-x^2(2-\rho_\eta^2)}{1-\rho_\eta^2}} + \frac{2xe^{-x^2}}{\sqrt{2-\rho_\eta^2}}\ Q\left(-\sqrt{\frac{2x^2}{1-\rho_\eta^2}}\right) \end{aligned} \tag{66}$$

Finally,

$$\begin{aligned} p(\zeta|\underline{\hat{\theta}}, H_\eta) &= p_{z_1}(.|H_\eta) \otimes p_{z_2}(.|H_\eta) \otimes \cdots \otimes p_{z_L}(.|H_\eta) \\ &= p(\zeta|H_\eta) \end{aligned} \tag{67}$$

where $\otimes$ is convolution. The last equation implies that given H_η, ζ and $\underline{\hat{\theta}}$ are independent.

D. Optimum Number of Diversity Branches in MRC

In this appendix we derive the optimal number of diversity branches for spectrum monitoring for the MRC receiver. It is clear that the efficacy of the proposed method relies on the statistics of the REC in the presence or absence of the PU. In particular, the performance of the algorithm improves if the emergence of the primary user causes a higher number of errors in each packet. Therefore we choose the number of diversity branches so as to maximize the difference between the average symbol error probabilities under H_1 and H_0. More specifically let

$$L_{\text{opt}} = \arg\max_L \mathfrak{D}(L) \tag{68}$$

where $\mathfrak{D}(L) \triangleq \bar{p}_1(L) - \bar{p}_0(L)$, and where $\bar{p}_\eta(L)$ for $\eta = 0, 1$ is the average (with respect to the channel coefficients) symbol error probability under H_η. Using the bound $Q(x) \leq 1/2e^{-x^2/2}$ we have,

$$\begin{aligned} \bar{p}_\eta(L) &= \int_0^\infty Q\left(\sqrt{2\gamma_\eta^{(\text{eff})}x^2}\right) \frac{2e^{-x^2}x^{2L-1}}{(L-1)!}dx \\ &\leq \frac{1}{(L-1)!}\int_0^\infty e^{-\gamma_\eta^{(\text{eff})}x^2}e^{-x^2}x^{2L-1}dx \\ &= \frac{1}{(L-1)!}\int_0^\infty x^{2L-1}\exp\left(-(1+\gamma_\eta^{(\text{eff})})x^2\right)dx \end{aligned} \tag{69}$$

Note that, [40],

$$\int_0^\infty x^m \exp(-\beta x^n)dx = \frac{\Gamma(\frac{m+1}{n})}{n\beta^{\frac{m+1}{n}}} \tag{70}$$

Thus we get

$$\bar{p}_\eta(L) \leq \frac{1}{(L-1)!}\frac{\Gamma(L)}{2(1+\gamma_\eta^{(\text{eff})})^L} = \frac{1}{2}(1+\gamma_\eta^{(\text{eff})})^{-L}. \tag{71}$$

Using the upper bound in (71) we get an approximation for $\mathfrak{D}(L)$. Assuming this approximation to be exact we get

$$\mathfrak{D}(L) = \frac{1}{2}\left((1+\gamma_1^{(\text{eff})})^{-L} - (1+\gamma_0^{(\text{eff})})^{-L}\right) \tag{72}$$

Treating L as a continuous variable, the derivative of $\mathfrak{D}$ with respect to L is given by

$$\begin{aligned} \frac{\partial\mathfrak{D}}{\partial L} =& \frac{1}{2}\Big(-(1+\gamma_1^{(\text{eff})})^{-L}\log(1+\gamma_1^{(\text{eff})}) \\ &+(1+\gamma_0^{(\text{eff})})^{-L}\log(1+\gamma_0^{(\text{eff})})\Big) \end{aligned} \tag{73}$$

Setting the derivative to zero and solving for L we get

$$\tilde{L} = \log\left(\frac{\log(1+\gamma_0^{(\text{eff})})}{\log(1+\gamma_1^{(\text{eff})})}\right) \Big/ \log\left(\frac{1+\gamma_0^{(\text{eff})}}{1+\gamma_1^{(\text{eff})}}\right) \tag{74}$$

Therefore, L_{opt} is obtained as either $\left\lfloor\tilde{L}\right\rfloor$ or $\left\lceil\tilde{L}\right\rceil$.

REFERENCES

[1] S. Chen, A. Wyglinski, R. Vuyyuru, and O. Altintas, "Feasibility analysis of vehicular dynamic spectrum access via queueing theory model," in *Vehicular Networking Conference (VNC), 2010 IEEE*, dec. 2010, pp. 223 –230.

[2] K. Tsukamoto, Y. Omori, O. Altintas, M. Tsuru, and Y. Oie, "On spatially-aware channel selection in dynamic spectrum access multi-hop inter-vehicle communications," in *Vehicular Technology Conference Fall (VTC 2009-Fall), 2009 IEEE 70th*, sept. 2009, pp. 1 –7.

[3] H. Li and D. Irick, "Collaborative spectrum sensing in cognitive radio vehicular ad hoc networks: Belief propagation on highway," in *Vehicular Technology Conference (VTC 2010-Spring), 2010 IEEE 71st*, may 2010, pp. 1 –5.

[4] J.-H. Chu, K.-T. Feng, C.-N. Chuah, and C.-F. Liu, "Cognitive radio enabled multi-channel access for vehicular communications," in *Vehicular Technology Conference Fall (VTC 2010-Fall), 2010 IEEE 72nd*, sept. 2010, pp. 1 –5.

[5] X. Y. Wang and P.-H. Ho, "A novel sensing coordination framework for cr-vanets," *Vehicular Technology, IEEE Transactions on*, vol. 59, no. 4, pp. 1936 –1948, may 2010.

[6] I. F. Akyildiz, W.-Y. Lee, M. C. Vuran, and S. Mohanty, "Next generation/dynamic spectrum access/cognitive radio wireless networks: A survey," *COMPUTER NETWORKS JOURNAL (ELSEVIER*, vol. 50, pp. 2127–2159, 2006.

[7] T. Yucek and H. Arslan, "A survey of spectrum sensing algorithms for cognitive radio applications," *Communications Surveys Tutorials, IEEE*, vol. 11, no. 1, pp. 116 –130, quarter 2009.

[8] D. Ariananda, M. Lakshmanan, and H. Nikoo, "A survey on spectrum sensing techniques for cognitive radio," in *Cognitive Radio and Advanced Spectrum Management, 2009. CogART 2009. Second International Workshop on*, may 2009, pp. 74 –79.

[9] B. Wang and K. Liu, "Advances in cognitive radio networks: A survey," *Selected Topics in Signal Processing, IEEE Journal of*, vol. 5, no. 1, pp. 5 –23, feb. 2011.

[10] J. Oh and W. Choi, "A hybrid cognitive radio system: A combination of underlay and overlay approaches," in *Vehicular Technology Conference Fall (VTC 2010-Fall), 2010 IEEE 72nd*, sept. 2010, pp. 1 –5.

[11] "Draft standard for wireless regional area networks," Mar. 2008.

[12] Y.-C. Liang, Y. Zeng, E. Peh, and A. T. Hoang, "Sensing-throughput tradeoff for cognitive radio networks," *Wireless Communications, IEEE Transactions on*, vol. 7, no. 4, pp. 1326 –1337, april 2008.

[13] L. Tang, Y. Chen, E. Hines, and M.-S. Alouini, "Effect of primary user traffic on sensing-throughput tradeoff for cognitive radios," *Wireless Communications, IEEE Transactions on*, vol. 10, no. 4, pp. 1063 –1068, april 2011.

[14] S. Akin and M. Gursoy, "Effective capacity analysis of cognitive radio channels for quality of service provisioning," *Wireless Communications, IEEE Transactions on*, vol. 9, no. 11, pp. 3354 –3364, november 2010.

[15] A. Hoang, Y.-C. Liang, and Y. Zeng, "Adaptive joint scheduling of spectrum sensing and data transmission in cognitive radio networks," *Communications, IEEE Transactions on*, vol. 58, no. 1, pp. 235 –246, january 2010.

[16] Q. Zhao, S. Geirhofer, L. Tong, and B. Sadler, "Opportunistic spectrum access via periodic channel sensing," *Signal Processing, IEEE Transactions on*, vol. 56, no. 2, pp. 785 –796, feb. 2008.

[17] S. Boyd and M. Pursley, "Enhanced spectrum sensing techniques for dynamic spectrum access cognitive radio networks," in *MILITARY COMMUNICATIONS CONFERENCE, 2010 - MILCOM 2010*, 31 2010-nov. 3 2010, pp. 317 –322.

[18] S. Boyd, J. Frye, M. Pursley, and T. Royster, "Spectrum monitoring during reception in dynamic spectrum access cognitive radio networks," *Communications, IEEE Transactions on*, vol. 60, no. 2, pp. 547 –558, february 2012.

[19] M. Orooji, E. Soltanmohammadi, and M. Naraghi-Pour, "Enhancing sensing-throughput tradeoff in cognitive radios using receiver statistics," submitted for publication.

[20] M. Naraghi-Pour and T. Ikuma, "Diversity techniques for spectrum sensing in fading environments," in *Military Communications Conference, 2008. MILCOM 2008. IEEE*, nov. 2008, pp. 1 –7.

[21] ——, "Autocorrelation-based spectrum sensing for cognitive radios," *Vehicular Technology, IEEE Transactions on*, vol. 59, no. 2, pp. 718 –733, 2010.

[22] A. Taherpour, M. Nasiri-Kenari, and S. Gazor, "Multiple antenna spectrum sensing in cognitive radios," *Wireless Communications, IEEE Transactions on*, vol. 9, no. 2, pp. 814 –823, february 2010.

[23] M. Orooji, R. Soosahabi, and M. Naraghi-Pour, "Blind spectrum sensing using antenna arrays and path correlation," *Vehicular Technology, IEEE Transactions on*, vol. 60, no. 8, pp. 3758 –3767, oct. 2011.

[24] R. Soosahabi, M. Orooji, and M. Naraghi-Pour, "Multi-antenna blind spectrum sensing for cognitive radios using path correlations," in *Global Telecommunications Conference (GLOBECOM 2011), 2011 IEEE*, dec. 2011, pp. 1 –5.

[25] R. Annavajjala and L. Milstein, "Performance analysis of linear diversity-combining schemes on rayleigh fading channels with binary signaling and gaussian weighting errors," *Wireless Communications, IEEE Transactions on*, vol. 4, no. 5, pp. 2267 – 2278, sept. 2005.

[26] D. Brennan, "Linear diversity combining techniques," *Proceedings of the IEEE*, vol. 91, no. 2, pp. 331 – 356, feb 2003.

[27] A. S. Tanenbaum and D. J. Wetherall, *Computer Networks*, 5th ed. Prentice Hall, 2010.

[28] K. Witzke and C. Leung, "A comparison of some error detecting crc code standards," *Communications, IEEE Transactions on*, vol. 33, no. 9, pp. 996 – 998, sep 1985.

[29] A. Leon-Garcia and I. Widjaja, *Communication Networks: Fundamental Concepts and Key Architectures*, 2nd ed. New York: McGraw Hill, 2004.

[30] G. Castagnoli, S. Brauer, and M. Herrmann, "Optimization of cyclic redundancy-check codes with 24 and 32 parity bits," *Communications, IEEE Transactions on*, vol. 41, no. 6, pp. 883 –892, jun 1993.

[31] P. Koopman, "32-bit cyclic redundancy codes for internet applications," in *Dependable Systems and Networks, 2002. DSN 2002. Proceedings. International Conference on*, 2002, pp. 459 – 468.

[32] R. Zhang, T. Lim, Y.-C. Liang, and Y. Zeng, "Multi-antenna based spectrum sensing for cognitive radios: A glrt approach," *Communications, IEEE Transactions on*, vol. 58, no. 1, pp. 84 –88, january 2010.

[33] D. Ramirez, G. Vazquez-Vilar, R. Lopez-Valcarce, J. Via, and I. Santamaria, "Detection of rank- signals in cognitive radio networks with uncalibrated multiple antennas," *Signal Processing, IEEE Transactions on*, vol. 59, no. 8, pp. 3764 –3774, aug. 2011.

[34] G. L. Stuber, *Principles of Mobile Communication*, 2nd ed. New York: Kluwer Accadempic Publishers, 2002.

[35] M. Gans, "The effect of gaussian error in maximal ratio combiners," *Communication Technology, IEEE Transactions on*, vol. 19, no. 4, pp. 492 –500, august 1971.

[36] A. Goldsmith, *Wireless Communications*, 1st ed. New York: Cambridge University Press, 2005.

[37] A. R. Webb, *Statistical Pattern Recognition*, 2nd ed. John Wieley

[38] W. C. Jakes, *Microwave Mobile Communications*, 2nd ed. New York: Wiley-IEEE Press, 1994.

[39] S. B. Wicker, *Error Control Systems for Digital Communication and Storage*, 1st ed. Upper Saddle River, New Jersey: Prentice-Hall, 1995.

[40] I. S. Gradshteyn and I. M. Ryshik, *Table of Integrals, Series, and Products*, 5th ed. London: Academic Press, 1994.

Erfan Soltanmohammadi (S'12) was born in Karaj, Iran, in 1984. He received the B.Sc. degree in electrical engineering from Khaje Nasir University of Technology (KNTU), Tehran, Iran, in 2007, and the M.Sc. degree from Amirkabir University of Technology (AUT), Tehran, Iran, in 2010. He is currently working toward the Ph.D. degree in systems (communication & signal processing) in the School of Electrical Engineering and Computer Science, Louisiana State University, Baton Rouge, Louisiana, U.S.A, where he is also a Graduate Research/Teaching Assistant. His current research interests include security in wireless sensor networks, cognitive radio, signal processing for communications, MIMO systems, and blind communication techniques.

Mahdi Orooji (S'11) was born in Tehran, Iran, in 1980. He received the B.Sc. degree in electrical engineering from University of Tehran in 2003. He is currently working toward the Ph.D. degree in the School of Electrical Engineering and Computer Science, Louisiana State University, Baton Rouge, Louisiana, USA. His research interests are wireless communication and statistical signal processing. Mr. Orooji received the Huel D. Perkins Doctoral Fellowship Award from LSU, 2009-2013.

Mort Naraghi-Pour (S'81-M'87) was born in Tehran, Iran, on May 15, 1954. He received the B.S.E. degree from Tehran University, Tehran, in 1977 and the M.S. and Ph.D. degrees in electrical engineering from the University of Michigan, Ann Arbor, in 1983 and 1987, respectively. In 1978, he was a student at the Philips International Institute, Eindhoven, The Netherlands, where he also did research with the Telecommunication Switching Group of the Philips Research Laboratories. Since August 1987, he has been with the School of Electrical Engineering and Computer Science, Louisiana State University, Baton Rouge, where he is currently an Associate Professor. From June 2000 to January 2002, he was a Senior Member of Technical Staff at Celox Networks, Inc., a network equipment manufacturer in St. Louis, MO. His research and teaching interests include wireless communications, broadband networks, information theory, and coding.

Dr. Naraghi-Pour has served as a Session Organizer, Session Chair, and member of the Technical Program Committee for many international conferences.